ECOLOGICAL MODELLING XXX (2006) XXX–XXX

available at www.sciencedirect.com

SCIENCE DIRECT®

journal homepage: www.elsevier.com/locate/ecolmodel

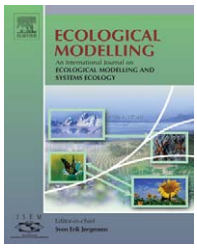

Integrating dynamic energy budgets into matrix population models

Tin Klanjscek[a,*], *Hal Caswell*[a], *Michael G. Neubert*[a], *Roger M. Nisbet*[b]

[a] *Biology Department, Woods Hole Oceanographic Institution MS#34, Woods Hole, MA 02543, USA*
[b] *Biological Sciences, Ecology, Evolution & Marine Biology, University of California Santa Barbara, Santa Barbara, CA 93106, USA*

ARTICLE INFO

Article history:
Received 8 February 2005
Received in revised form
3 December 2005
Accepted 1 February 2006

Keywords:
Dynamic energy budget (DEB)
Matrix population
Model
Integration
Supply-side
Food availability

ABSTRACT

Population dynamics depend on the growth and reproduction of individuals, which are dictated by energy intake and budgeting. Here we show how to construct a simple matrix population model from a dynamic energy budget model in a constant or seasonally variable environment. The matrix model accurately predicts asymptotic population dynamics for a wide range of parameter values and environmental conditions. The model captures some transients well, but more elaborate stage structure is necessary when the initial age distribution within stages is far from the stable age distribution.

1. Introduction

Food availability and the resulting energy intake and budgeting are major factors affecting growth and reproduction of individuals and, therefore, population dynamics. To investigate these effects, one needs demographic models that incorporate energy budgeting. In this paper, we use a physiological model describing individual energy acquisition, energy allocation, growth and reproduction to calculate the vital rates of a simple demographic model.

When constructing such coupled energy budget/demographic models, one must make two choices. First, one must choose a description of the energy budget of an individual. We chose a simple model based on the most comprehensive mathematical theory currently available: the dynamic energy budget (DEB) theory (Kooijman, 2000; see Section 1.1). This model has the advantage of being a "supply-side model" in which food availability determines growth, survival and reproduction. As such it enables one to analyze the interacting effects of physiology and environmental variability on population dynamics—effects that we hope to study in the future.

Second, one must pick a framework for describing the demography. Previous theoretical studies have used continuous-time ordinary, delay, or partial differential equations for this purpose. This is a mathematically natural choice because energy budget models typically treat time as continuous variable. Practical or biological circumstances, however, often make discrete-time matrix population models more convenient, hence their frequent use in empirical population ecology (Caswell, 1989, 1996; Ripley and Caswell, in press). Despite their popularity, we know of no supply-side energy bud-

* *Corresponding author*. Tel.: +1 5082893628.
E-mail address: tin@whoi.edu (T. Klanjscek).

0304-3800/$ – see front matter © 2006 Elsevier B.V. All rights reserved.
doi:10.1016/j.ecolmodel.2006.02.023

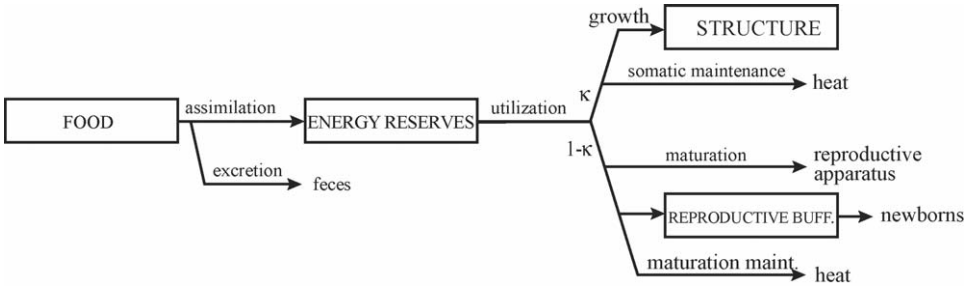

Fig. 1 – The fluxes of energy in a κ-rule DEB model. Energy from food is assimilated, stored into energy reserves, and then utilized. A proportion κ of the utilized energy is spent on growth and somatic maintenance. A proportion $(1-\kappa)$ is either spent on maturation and maturation maintenance, or stored into a reproductive buffer and spent on reproduction. In case of energy shortage, the somatic maintenance has the absolute priority in energy allocation. Boxed compartments are explicitly modeled in the DEB. Structure and newborns, although not measured in units of energy, represent sinks of energy.

get model linked with a matrix population model. Here, we have chosen a simple two-stage matrix model (described in Section 1.2) for our demographic model partly to demonstrate how to make such a link (in Section 2). We provide a recipe for linking more general energy budget models with more general matrix population models in Appendix A.

In Section 3 we compare our model's demographic predictions to simulations of an individual based model (IBM) in which individuals are governed by the same physiological model. It turns out that the model accurately captures both long and short-term population dynamics when the population is initially close to the stable age distribution. When the population is not initially close to the stable age distribution, our model and the IBM may disagree; we describe the reasons for this disagreement, and how it can be ameliorated, in Section 4.

1.1. *The DEB model*

Energy budget models describe the acquisition and utilization of energy by individuals for maintenance, growth and reproduction (e.g. Ren and Ross, 2001). We constructed a simple DEB model based on Kooijman (2000) and Muller and Nisbet (2000). The model describes the energy budget of an ectothermic organism that grows, matures at a fixed size, and reproduces in discrete periodic events during the breeding season (birth-pulse reproduction). For a comprehensive review of DEB models and their applications, see Nisbet et al. (2000).

In this DEB model, the organism is partitioned into two compartments: structure and energy reserves. The exact composition of these compartments depends on the species. In general, the reserves are materials that can be utilized as an energy source by the organism (e.g. non-structural lipids, glucose and some proteins). The remaining tissue (e.g. bones, muscle, structural lipids, etc.) compose the structure compartment. Fueled by the energy from the reserves, the structure enables the organism to interact with its environment and feed.

Organisms assimilate acquired food into the energy reserves, or excrete it as feces. They utilize energy at a rate determined by the energy stored in the reserves. According to Kooijman's "κ-rule" (Kooijman, 2000), organisms allocate a fraction κ of the utilized energy to growth and somatic maintenance (i.e. increase and maintenance of the structure), and the remaining fraction to maturation or reproduction, and to maintaining the acquired level of maturity (Fig. 1). Somatic maintenance takes precedence over any other energy need. If the energy that can be extracted from the reserves is not sufficient to satisfy the somatic maintenance, the organism dies.

We use V (structural volume) and e (energy density $[E]$ relative to maximum energy density $[E_m]$) as state variables that describe the structure and reserves of an individual of age s. Throughout the text we simplify the discussion by treating V as a measure of the size of the structure of the organism. See Table 1 for a description of all the state variables and parameters of the model, and Table 2 for the parameter values we used as a starting point for our analyzes. A sample solution of the DEB model is given in Fig. 2.

1.1.1. *Growth*

The rate of energy intake f, which is measured relative to its maximum value, is a function of food availability ((Kooijman, 2000). The rate of change of scaled reserve density, e, is proportional to the difference between f and e, where the constant of proportionality v is called the energy conductance:

$$\frac{de}{ds} = v(f-e)V^{-1/3}. \tag{1}$$

The rate of increase of structure in DEB theory is determined by the energy allocated to growth and somatic maintenance, after the somatic maintenance has been met:

$$\frac{dV}{ds} = \max\left(\frac{mg}{e+g}(eV_m^{1/3}V^{2/3}-V), 0\right). \tag{2}$$

Note that the size of the structure cannot decrease.

1.1.2. *Reproduction*

We assume that the organism is mature, and allocates energy to reproduction, whenever $V \geq V_p$. In mature organisms, the energy flux to reproductive processes (including maturation) is

$$E_R = \begin{cases} (1-\kappa)[E_m]\frac{eg}{e+g}(vV^{2/3}+mV) & \text{when } \frac{dV}{ds} > 0 \\ [E_m](veV^{2/3}-mg\kappa V) & \text{when } \frac{dV}{ds} = 0, \end{cases} \tag{3}$$

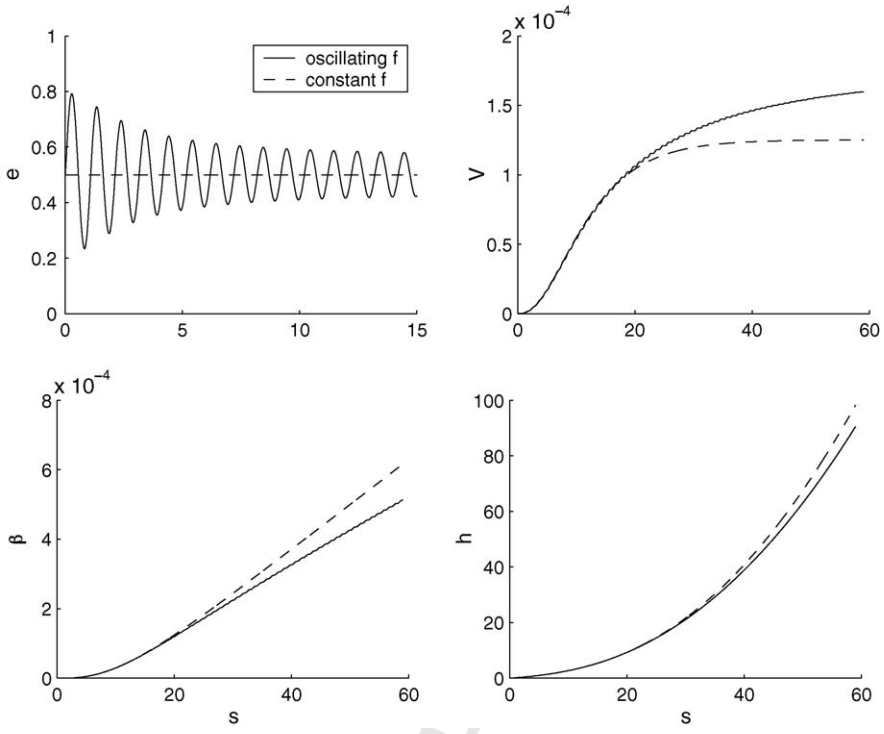

Fig. 2 – Sample solutions of the DEB model as a function of age (*s*) using the parameter values from Table 2 for constant energy intake ($f(s) = 0.5$) and oscillating energy intake ($f(s) = 0.5 + 0.3\sin(2\pi s)$). In the fluctuating environment, the organism grows larger, commits less energy to reproduction, and accumulates less damage (lower $h(s)$). For additional discussion see Muller and Nisbet (2000).

and the energy flux required to maintain maturity is

$$E_M = (1-\kappa)[E_m]mgV_p. \quad (4)$$

Hence, the flux of energy to the reproduction buffer (β) is

$$\frac{d\beta}{ds} = \max(E_R(V) - E_M, 0). \quad (5)$$

We assume that the energy buffer is emptied and utilized for reproduction at each breeding event, if the mother accumulated enough energy to produce at least one newborn.

1.1.3. *Mortality*

Probability that the organism dies by age $s + ds$, given that it survived until age s, is proportional to the hazard rate $h(s)$:

$$P(\text{dead at } s + ds | \text{alive at } s) = h(s)\,ds. \quad (6)$$

The hazard rate increases at a rate proportional to the density of damage-inducing compounds within the organism (Q/V):

$$\frac{dh(s)}{ds} = h_a\frac{Q}{V}. \quad (7)$$

Damage inducing compounds are generated by respiration:

$$\frac{dQ}{ds} = \eta g[E_m]\left(\frac{dV}{ds} + mV\right). \quad (8)$$

Since $h(s)$ is proportional to both η and h_a, we can simplify analysis if assume that η is unity and vary only h_a in the analyses. The hazard rate and the mass of damage-inducing compounds are assumed negligible in a newborn individual, so we set these variables to zero at birth.

Throughout the paper we use the parameter values mostly obtained from a DEB model for the mussel *Mytilus edulis* (Table 2) (Muller and Nisbet, 2000). The value for $[E_m]$ was not available in Muller and Nisbet (2000); we choose the one that approximately matches the median value used by Fujiwara et al. (2004).

1.2. *The matrix population model*

Matrix population models are discrete-time structured models that divide population into discrete stages, and describe evolution of the population through these stages through time:

$$\mathbf{n}(t+\alpha) = \mathbf{A}\mathbf{n}(t). \quad (9)$$

$\mathbf{A}$ is a projection matrix, α is the projection interval, and the vector $\mathbf{n}(t)$ gives the distribution of individuals among stages at time t.

Although most applications require more complicated structures, as a test case we used a two-stage matrix model that distinguishes between immature and mature individuals. Individuals become mature when they reach a minimal reproductive size (V_p).

The projection matrix is

$$\mathbf{A} = \begin{bmatrix} P_{11} & F \\ P_{21} & P_{22} \end{bmatrix}. \quad (10)$$

Table 1 – State variables as a function of age (s) and parameters of the DEB model. For further discussion see Kooijman (2000)

Descriptor	Dimension	Description
$V(s)$	Length^3	Volume of the structure compartment
$[E_m]$	Energy/length^3	Maximum energy reserve density
$[E]$	Energy/length^3	Energy reserve density
$e(s)$	–	Scaled energy density in the energy reserves, $\frac{[E]}{[E_m]}$
$\beta(s)$	Energy	Cumulative energy committed to reproduction
$Q(s)$	Mass	Mass of damage-inducing compound
$h(s)$	Probability/time	Hazard rate: probability of death per unit of time
κ	–	Energy partitioning coefficient
κ_R	–	Fraction of reproduction energy realized in a newborn
v	Length/time	Energy conductance
m	Time^{-1}	Maintenance rate coefficient: cost of maintenance relative to cost of growth
g	–	Energy investment ratio: cost of growth relative to maximum avail energy for growth
η	Mass/energy	Mass–energy coupler: damage-inducing compound accumulated per energy respired
V_b	Length^3	Structural volume at birth
V_p	Length^3	Structural volume at maturation
V_m	Length^3	Maximum structural volume $\left(\frac{v}{mg}\right)^3$
C_N	Energy	Effective energy cost of a newborn female
h_a	Probabability length^3/mass time	Ageing acceleration—rate of increase of the hazard rate
f	–	Energy intake scaled to maximum energy intake

Table 2 – Standard parameter values

Parameter	Value
κ	0.8
κ_R	0.001
v	0.075 m y^{-1}
m	0.58 y^{-1}
g	0.25
V_b	10^{-9} m^3
V_p	1.73×10^{-6} m^3
$[E_m]$	0.7 aJ[a]
h_a	0.15 m^3 d$_{DNA}^{-1}$ y^{-1}[b]
f	0.5

[a] Converts a chosen proxy for energy (dry weight in Muller and Nisbet (2000)) into Joules, and cancels out after parameterization (Fujiwara et al., 2004).

[b] d_{DNA} is a unit of the damage-inducing compound which cancels out in calculations.

We assumed a birth-pulse population, with births occurring at the end of the projection interval. The transition probabilities depend on γ, the maturation probability, and on σ_1 and σ_2, the survival probabilities in stages 1 and 2:

$$P_{11} = \sigma_1(1-\gamma), \tag{11}$$

$$P_{21} = \sigma_1\gamma, \tag{12}$$

$$P_{22} = \sigma_2. \tag{13}$$

We assume that the maturation probability is independent of survival, and that the projection interval is less than the age at maturity.

If all vital rates are constant, the asymptotic growth rate of the population is given by the dominant eigenvalue λ_1 of the projection matrix **A**, and the intrinsic rate of increase is

$$r = \frac{1}{\alpha}\ln\lambda_1. \tag{14}$$

The stable stage distribution is given by the right eigenvector $\mathbf{w}_1$ associated with λ_1. Other demographic statistics that can be obtained from the model include the reproductive value ($\mathbf{v}_1$, the left eigenvector associated with λ_1), and sensitivities of the growth rate to changes of the elements in the matrix.

2. Methods

In this section we derive the matrix model from solutions of the DEB model. We assume that food availability $f(t)$ is either constant or periodic with a period equal to the projection interval (this might represent seasonal variability, for example).

Under these assumptions the age (s) of an individual completely determines its size, the contents of its reproductive buffer, and how likely it is to die.

Individuals of different ages within each stage of the matrix model have different probabilities of survival and rates of growth and reproduction. Hence, the parameters for each stage are a weighted average of the DEB solutions. We use the stable age distribution within a stage as the weighting function, although this will be strictly correct only when the distribution is stable.

The stable age distribution is

$$\phi(s) = K\lambda_1^{-s/\alpha}\exp\left(-\int_0^s h(\xi)\,d\xi\right), \tag{15}$$

where K is the ratio of number of newborns to the total population size in the stable age distribution (see Appendix B).

2.1. *Maturation probability* (γ)

Growth in the DEB model is deterministic. Since the period of food availability is equal to one projection interval, all individuals experience the same food at the same age and, consequently, reach the reproductive size (V_p) and become mature at the same age, τ_p. Therefore, organisms in stage i are of age $s \in [\tau_i, \tau_{i+1})$. In our matrix model, $\tau_1 = 0$, $\tau_2 = \tau_p$ and $\tau_3 = \infty$.

We have assumed that organisms cannot grow from birth to maturity in less than one projection interval, so we restrict

our attention to

$$\tau_p \geq \alpha. \tag{16}$$

Therefore, given that they survive, all individuals in stage i with ages:

$$(\tau_{i+1} - \alpha) \leq s < \tau_{i+1} \tag{17}$$

will grow into stage $i+1$ in one projection interval. The probability of growing from stage i into the next stage, conditioned on survival, is therefore

$$\gamma_{i+1,i} = \frac{\int_{\tau_{i+1}-\alpha}^{\tau_{i+1}} \phi(s)\,ds}{\int_{\tau_i}^{\tau_{i+1}} \phi(s)\,ds}. \tag{18}$$

In our matrix model, individuals can only mature from the immature to the mature stage. Hence, the maturation probability:

$$\gamma = \frac{\int_{\tau_p-\alpha}^{\tau_p} \phi(s)\,ds}{\int_0^{\tau_p} \phi(s)\,ds}. \tag{19}$$

2.2. *Survival probabilities* (σ)

Individuals in stage i at time t have age $s \in [\tau_i, \tau_{i+1})$. We assume their age distribution is $\phi(s)$. After one projection interval, all individuals grow older by α and have the distribution $\phi(s)e^{r\alpha}$. Survivorship is given by the ratio of number of individuals who lived through the projection interval and the initial number of individuals:

$$\sigma_i = \frac{\int_{\tau_i+\alpha}^{\tau_{i+1}+\alpha} \phi(s)e^{r\alpha}\,ds}{\int_{\tau_i}^{\tau_{i+1}} \phi(s)\,ds}, \tag{20}$$

$$\sigma_i = \lambda_1 \frac{\int_{\tau_i+\alpha}^{\tau_{i+1}+\alpha} \phi(s)\,ds}{\int_{\tau_i}^{\tau_{i+1}} \phi(s)\,ds}. \tag{21}$$

2.3. *Fecundity* (F)

We estimate the flux of energy to the reproductive buffer as the average flux within the stage:

$$\overline{\Delta\beta_i} = \alpha \frac{\int_{\tau_i}^{\tau_{i+1}} \phi(\xi) \left.\frac{d\beta(s)}{ds}\right|_{s=\xi} d\xi}{\int_{\tau_i}^{\tau_{i+1}} \phi(s)\,ds}. \tag{22}$$

If C_N is the energy cost of a newborn, one adult produces:

$$N_2 = \frac{\overline{\Delta\beta_2}}{C_N} \tag{23}$$

newborn females on average during each breading season. Considering both energetics and demography, the energetic cost of one newborn female is

$$C_N = \frac{1}{\kappa_R}[E_m](\kappa g + e)V_b. \tag{24}$$

This cost includes the energy used to create its structure (proportional to $[E_m]V_b$), the energy given to it by its mother ($e[E_m]V_b$). Furthermore, there is a cost associated with the tissue mother discards at birth, and the demographic reality that only a fraction of newborns are female and survive. This cost is represented by $\kappa_R \in (0, 1]$ in Eq. (24).

Our model ignores respiration of the structure of the newborn prior to birth, possibly variable duration of pre-natal development and other less significant factors. The form we use is simple, but still elaborate enough to capture the increase in energy transfer from mother to child as the energy density of the mother (e) increases. We assumed that the young were born with energy density equal to the mother's averaged over the projection interval.

Fecundity (F) is the number of newborns at time $t+\alpha$ per adult at time t. In our birth-pulse population, it is the rate of production of newborns per adult that survived to the end of the projection interval α (Caswell, 2001, pp. 172–173):

$$F = \sigma_2 N_2. \tag{25}$$

Eqs. (19), (21) and (25) provide the necessary vital rates to write down the projection matrix (10). However calculating $\phi(s)$ requires a value for λ_1. We can arrive at λ_1 through an iterative process: start with $\lambda_1 = 1$, find the matrix model and calculate the growth rate λ_1'. Repeat the process with $\lambda_1 = \lambda_1'$ until the desired accuracy is reached (Caswell, 2001, p. 164). In this paper we required that the growth rate converge to the accuracy of 10^{-3}.

2.4. *The individual-based model (IBM)*

To assess the ability of the matrix model to capture the dynamics of a population, we compared its asymptotic and transient dynamics with the simulations of an individual based model (IBM) in which individuals grow according to the DEB (Fig. 3).

In the IBM, at each time step individuals of age s grow older by ds, grow by dV, die with probability $h(s)$ds, and commit $d\beta(s)$ energy to reproduction. Every projection interval (α units of time) individuals reproduce according to the energy stored in the reproductive buffer.

We calculated the number of newborn females produced by one individual female in one breeding season (N) from the ratio of the energy accumulated since the last reproduction ($\Delta\beta$)

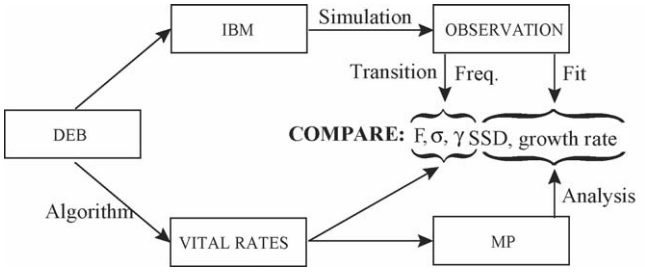

Fig. 3 – Schematic of the assessment process. We created an IBM based on the DEB model. We fitted the growth rate and stable stage distribution (SSD) to the observed population dynamics, and used the transition frequencies observed in a simulation of the IBM to calculate the observed vital rates. At the same time, we arrived at the vital rates through the methods described in Sections (2.1)–(2.3) and calculated the growth rate and SSD from the resulting MP model. The performance of the matrix model has been assessed through comparison between the two sets of vital rates, growth rates and SSDs.

and the energy needed to produce one newborn female (C_N). The ratio is not an integer, whereas N needs to be. Therefore, we have to round the ratio so that the expected number of newborns is equal to it. Denoting the integer part of the ratio as $\text{floor}\left(\frac{\Delta\beta}{C_N}\right)$, the number of female newborns for each individual is

$$N = \begin{cases} \text{floor}\left(\frac{\Delta\beta}{C_N}\right)+1 & \text{with probability } \left(\frac{\Delta\beta}{C_N} - \text{floor}\left(\frac{\Delta\beta}{C_N}\right)\right) \\ \text{floor}\left(\frac{\Delta\beta}{C_N}\right) & \text{with probability } \left(1 - \left(\frac{\Delta\beta}{C_N} - \text{floor}\left(\frac{\Delta\beta}{C_N}\right)\right)\right) \end{cases}. \tag{26}$$

We eased the computational requirements by treating individuals with age differences less than ds = 0.01 as having the same age. Because reproduction is seasonal, and all individuals reproduce at the same time, the resulting age distribution is 'spiked', i.e. individuals can have only discrete ages corresponding to the reproductive events. This is in contrast with the continuous age distribution that has been assumed in the matrix model.

From the IBM simulations, we measured population growth rate and the stable stage distribution (SSD) and compared them to those predicted by the matrix model. We also measured σ_1, σ_2, and γ from the the IBM. Let the number of transitions from stage j to stage i be n_{ij}, where stages 1, 2, and 3 are immature, mature and dead individuals, respectively (Table 3). Then

$$\hat{\sigma}_1 = 1 - \frac{n_{31}}{n_{11}+n_{21}+n_{31}}, \tag{27}$$

$$\hat{\sigma}_2 = 1 - \frac{n_{32}}{n_{22}+n_{12}+n_{32}}, \tag{28}$$

$$\hat{\gamma} = \frac{n_{21}}{n_{11}+n_{21}}, \tag{29}$$

$$\hat{F} = \frac{n_{12}}{n_{22}+n_{32}}. \tag{30}$$

The asymptotic comparisons of the rates and demographic statistics required that the population converge to a stable age distribution. We ran the simulations for 130 units of time or until the population went extinct. We discarded the first 10% and the last 20% of the simulated time interval to allow for as much convergence as possible before the onset of low-number effects, and used the remaining data as observations for comparison. We expedited convergence by using the Eq. (15) to distribute the initial 1000 individuals through ages using the predicted λ_1. The convergence, however, was not always attained, especially for parameter values that produced very small growth rates. If the initial 1000 individuals did not a provide sufficient number of observations to measure the vital rates, we used an initial population of 10^6 individuals.

3. Results

3.1. *Long term (asymptotic) dynamics*

In Table 4 we compare observations of the IBM and the predictions of the matrix model for the standard parameter values listed in Table 2 for $\tau_p = 3\alpha$.

Table 3 – Transition counts n_{ij} from stage j to stage i

	Immature ($j = 1$)	Mature ($j = 2$)
Immature ($i = 1$)	Immature that did not mature (n_{11})	Newborns (n_{12})
Mature ($i = 2$)	Immature that matured (n_{21})	Mature that survived (n_{22})
Dead ($i = 3$)	Immature that died (n_{31})	Mature that died (n_{32})

Table 4 – Comparison of predicted and observed demographic statistics and vital rates

	Observed	Predicted
λ	1.13	1.13
SSD	0.61	0.59
γ	0.26	0.26
σ_1	0.93	0.91
σ_2	0.84	0.72
F	0.71	0.77

Predicted and observed γ and σ_1 agree extremely well; even the greatest proportional differences[1], for F and σ_2, are less than 12%. As a result, the growth rates hardly differ. To see whether these demographic statistics obtained from the matrix model and the IBM agree for a wide range of parameters, we compared the observed and predicted demographic statistics for different values of the parameters h_a, f, C_N, κ, E_m and α. Unless noted otherwise, while changing one parameter, we used values from Table 2 for others.

The results are shown in Figs. (4)–(9). Plot A of each figure compares the growth rates. Plots B and C show proportional differences between predicted and observed growth rates, stable stage distributions, fecundities, and transition probabilities. Plot D shows the proportional differences between the observed and predicted survival probabilities.

Population growth rates match very well across all the parameter ranges investigated. The estimates of the vital rates show greatest discrepancies for low growth rates, mainly because populations went extinct in the IBM before reliable observation could be made.

Fecundity was, in general, overestimated. This is notable in Fig. 4 for large hazard rates: F is overestimated by as much as 7% for $h_a = 0.1$ and more than 100% for large h_a. The main reason for the overestimate is that when h_a is high, individuals in the IBM die before they accumulate enough energy to reproduce, and whatever they have accumulated is lost to the population. The matrix model, however, pools the energy committed to reproduction from all adults, so the accumulated energy for reproduction is not lost. We call this the pooling effect.

The pooling effect is ubiquitous, but more notable when adult life span is short and when it takes longer to accumulate enough energy to reproduce, i.e. when h_a, C_N and $[E_m]$ are large,

[1] proportional difference $= \frac{\text{observed value} - \text{predicted value}}{\text{observed value}}$.

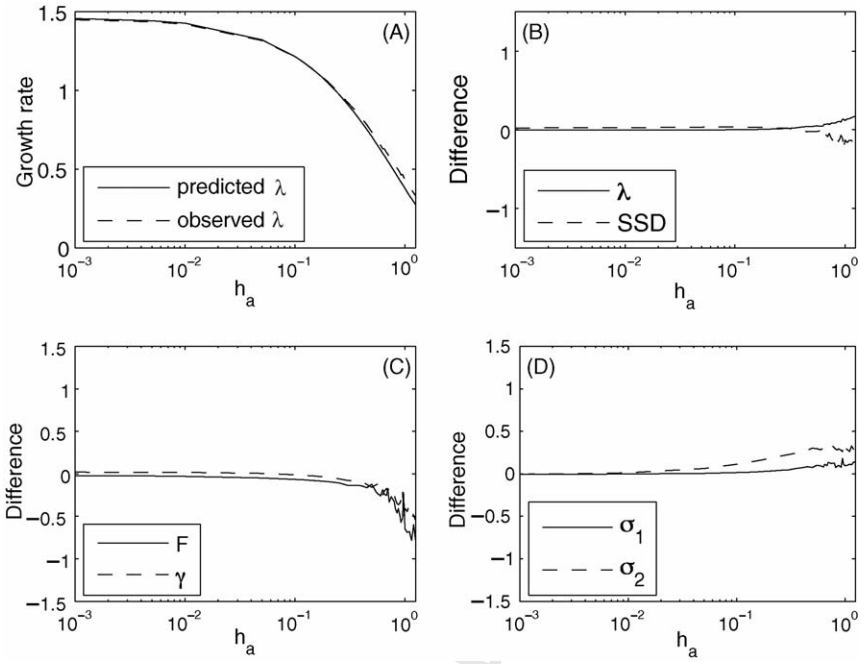

Fig. 4 – Predicted and observed vital rates and demographic statistics vs. ageing acceleration (h_a): the comparison of growth rates (A), proportional difference between the predicted and observed λ and SSD (B), *F* and γ (C), and σ_1 and σ_2 (D). For $h_a < 10^{-3}$ the agreement continued to be excellent (tested to $h_a = 10^{-5}$).

and f and κ are small. Since all of these factors decrease the population growth rate, the pooling effect is also more notable for small growth rates.

Figs. 5 and 7 provide further examples of the pooling effect. In Fig. 5, we overestimate fertility by about 80% for small f (and small growth rates). In Fig. 7, the same happens for large $[E_m]$.

In Fig. 6 we changed the cost of newborns C_N by changing the reproductive efficiency κ_R (24). For very large C_N, both the observed and the predicted growth rates asymptote to the

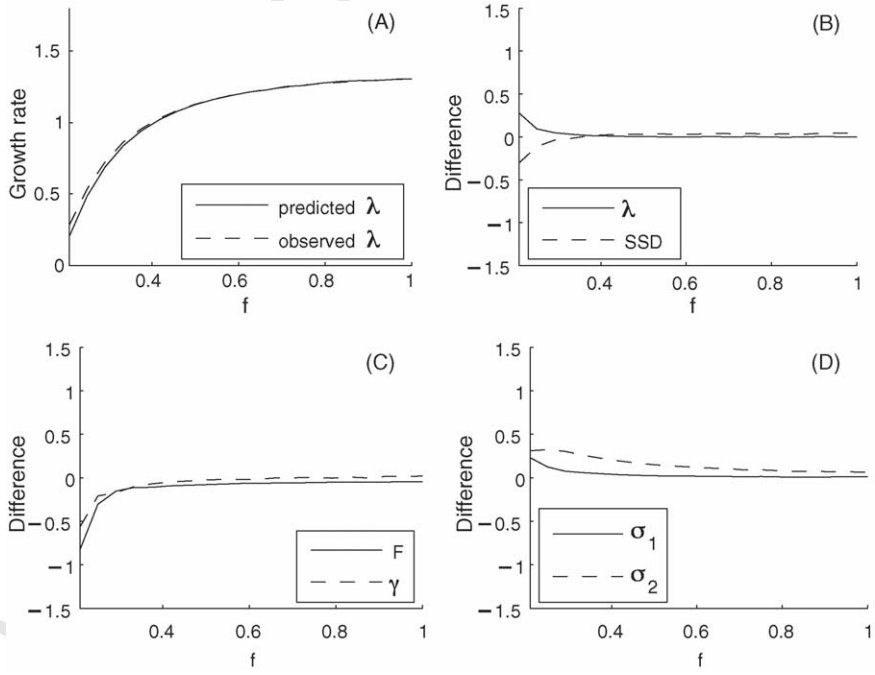

Fig. 5 – Predicted and observed vital rates and demographic statistics vs. energy intake (f): the comparison of growth rates (A), proportional difference between the predicted and observed λ and SSD (B), *F* and γ (C), and σ_1 and σ_2 (D). For $f < 0.2$ populations went extinct too fast to estimate vital rates from observations.

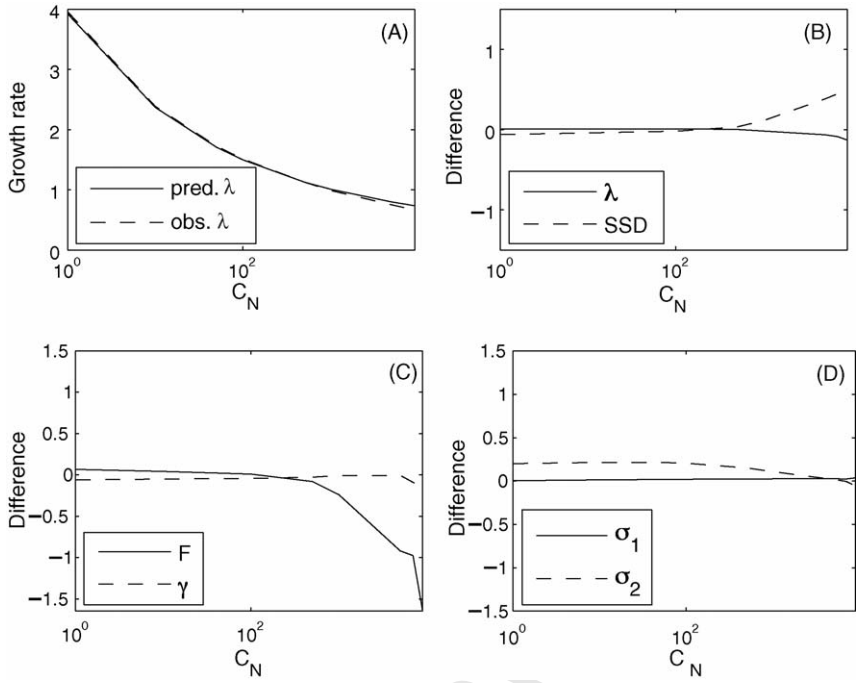

Fig. 6 – Predicted and observed vital rates and demographic statistics vs. cost of a newborn (C_N): the comparison of growth rates (A), proportional difference between the predicted and observed λ and SSD (B), *F* and γ (C), and σ_1 and σ_2 (D).

growth rate dictated by mortality alone ($\lambda \approx 0.7$). Although it should remain constant, the observed survivorship of adults ($\hat{\sigma}_2$) changes with C_N. It is not clear why $\hat{\sigma}_2$ changes, but huge growth rate and finite possible age of adults are probable causes. When the number of individuals is large and increases quickly, significant rounding due to limited number of digits represented in the computer takes place, influencing the transition counts (n_{ij} in (27)–(30)) and the observed vital rates. Furthermore, when the population is huge, a large number of individuals live to very old age. Consequently, the maximum

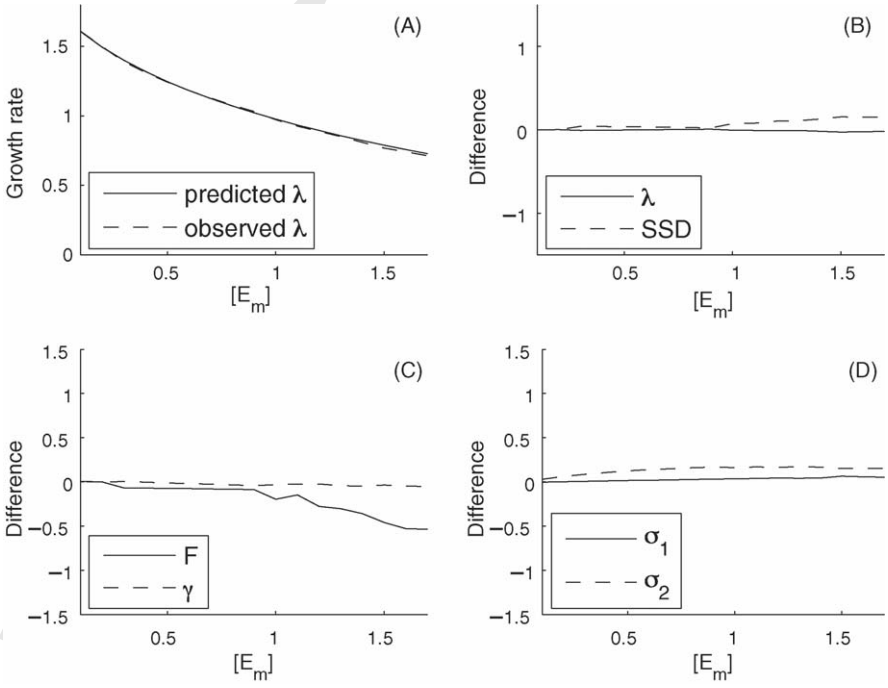

Fig. 7 – Predicted and observed vital rates and demographic statistics vs. maximum energy density ($[E_m]$): the comparison of growth rates (A), proportional difference between the predicted and observed λ and SSD (B), *F* and γ (C), and σ_1 and σ_2 (D). The range was adopted from Fujiwara et al. (2004).

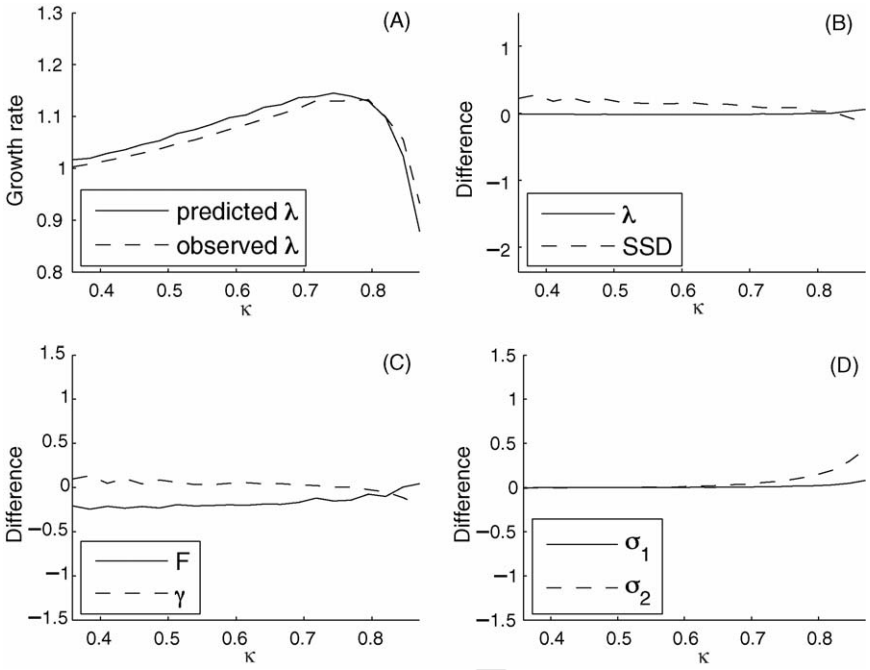

Fig. 8 – Predicted and observed vital rates and demographic statistics vs. energy allocation ratio (κ): the comparison of growth rates (A), proportional difference between the predicted and observed λ and SSD (B), F and γ (C), and σ_1 and σ_2 (D).

possible age assumed in the IBM may not be adequate: some individuals may be assumed dead just because they exceed the maximum age assumed by the IBM, thereby increasing adult mortality (decreasing $\hat{\sigma}_2$).

The fraction of energy used for growth and somatic maintenance (κ) is probably the most important parameter in the DEB theory. In Fig. 8 we changed κ to represent a range of organisms, from reproduction-oriented (small κ) to growth-oriented (large κ). We observed the greatest discrepancies in the stable stage distribution (up to 25% for small κ), mostly due to similarly large overestimate of fecundity due to the pooling effect.

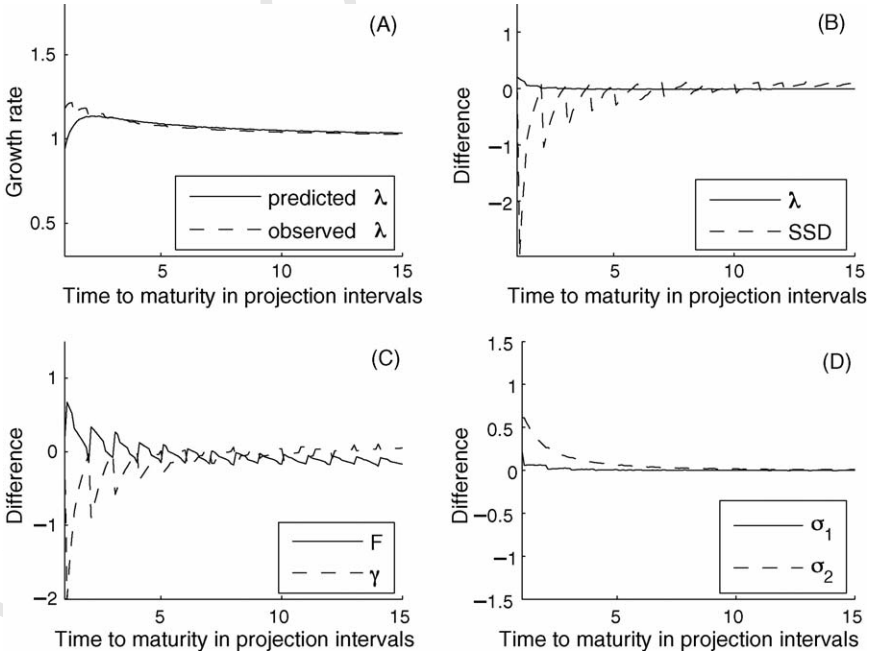

Fig. 9 – Predicted and observed vital rates and demographic statistics vs. age to maturity measured in projection intervals (α): the comparison of growth rates (A), proportional difference between the predicted and observed λ and SSD (B), F and γ (C), and σ_1 and σ_2 (D).

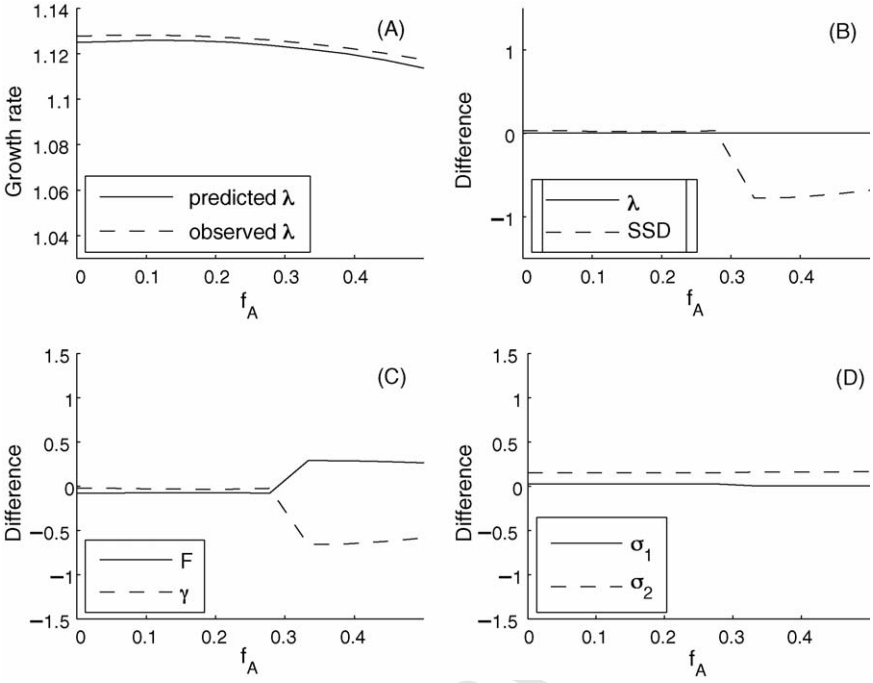

Fig. 10 – Predicted and observed vital rates and demographic statistics vs. amplitude of sinusoidal food intake fluctuations (f_A): the comparison of growth rates (A), proportional difference between the predicted and observed λ and SSD (B), F and γ (C), and σ_1 and σ_2 (D).

We varied the relationship between the projection interval and the age at maturity by changing the length of the projection interval (Fig. 9). A shorter projection interval implies a longer time to maturity measured in projection intervals because the growth of organisms measured in units of time (from the DEB model) is not affected by the chosen projection interval (α). The observed ratio of mature to immature individuals shows a sawtooth pattern as the time to maturity deviates from integer multiple of the projection interval.

This is a consequence of spiked age distributions characteristic of birth-pulse populations (discussed in Section 2.4). Changing the projection interval changes the ages at which spikes occur at the census time, while the age at maturity always stays the same. The interaction between the two can influence transition counts. For example, if time to maturity is 2.00 projection intervals, a cohort of newborns is counted as mature two censuses later. If the time to maturity is 2.01 projection intervals, the cohort is counted as immature. Neither cohort produces any newborns. Therefore, one can expect large discrepancies when comparing the ratios of individuals in each stage as the time to maturity changes, but not when comparing population-level statistics, such as the growth rate.

3.2. *Seasonal environmental variability*

In many systems, the environment varies strongly between any 1 year, but there is little year to year variations for any given season. Most long-lived organisms have ways of coping with that variability, e.g. energy reserves to carry them through times of scarcity. In this section, we ask if the matrix model can successfully account for such variability. We do this by varying the energy intake f in our DEB model and then assessing its effects on the population growth rate.

If we assume that the projection interval represents 1 year we can represent seasonal variability by a periodic energy intake with period equal to 1 year:

$$f(t) = f_0 + f_A \sin\left(\frac{2\pi}{\alpha} t\right), \tag{31}$$

with f_A representing the amplitude of oscillations, and average energy intake $f_0 = 0.5$.

We calculated population growth rates (Fig. 10) for the range of f_A from the minimum (constant energy intake, $f_A = 0$) to the maximum ($f_A = f_0$). We assumed that the newborns are born with the average energy density ($e(0) = 0.5$) in the calculations; this assumption guarantees that all individuals follow the same developmental path.

The abrupt changes of the proportional differences in SSD, F and γ in Fig. (10) at $f_A \simeq 0.3$ are due to a sudden increase in the observed fecundity and decrease in the observed transition probability as the seasonal variability increases above $f_A > 0.3$. Even though the predicted vital rates do not follow that trend, the predicted and observed population growth rates agree well over the whole range of f_A.

The growth rate is highest when the seasonal variability is limited, and lowest when the seasonal variability is extreme. In a variable environment, both the energy committed to reproduction and the hazard rate are smaller than in a constant environment (Fig. 2). For small seasonal variability the benefits of a smaller hazard rate outweigh the detriments of a smaller commitment of energy to reproduction; the reverse holds for large seasonal variability.

3.3. *Short-term (transient) dynamics*

To assess accuracy of the matrix model for predicting transient dynamics we examined two sets of scenarios, loosely corresponding to colonizations and catastrophes. In the colonization scenarios, we initialized the IBM with 1000 newborns or with 1000 individuals that had just matured. In the catastrophe scenarios, we allowed the population to converge for 20 projection intervals and then eliminated all the juveniles or all the mature individuals. We used the standard parameters (Table 2).

Age distributions extremely different from the stable age distribution in the colonization scenarios proved to be a significant challenge to the simple two-stage matrix model. Two effects cause the large discrepancies in transients when newborns only are considered: the pooling effect and the numerical diffusion. The pooling effect, discussed in Section 3.1, results from the ability of the adults in the matrix model to pool their reproductive resources and produce newborns immediately, while in reality individuals must accumulate enough energy to reproduce. The numerical diffusion is a consequence of the inability of the matrix model to distinguish individ-

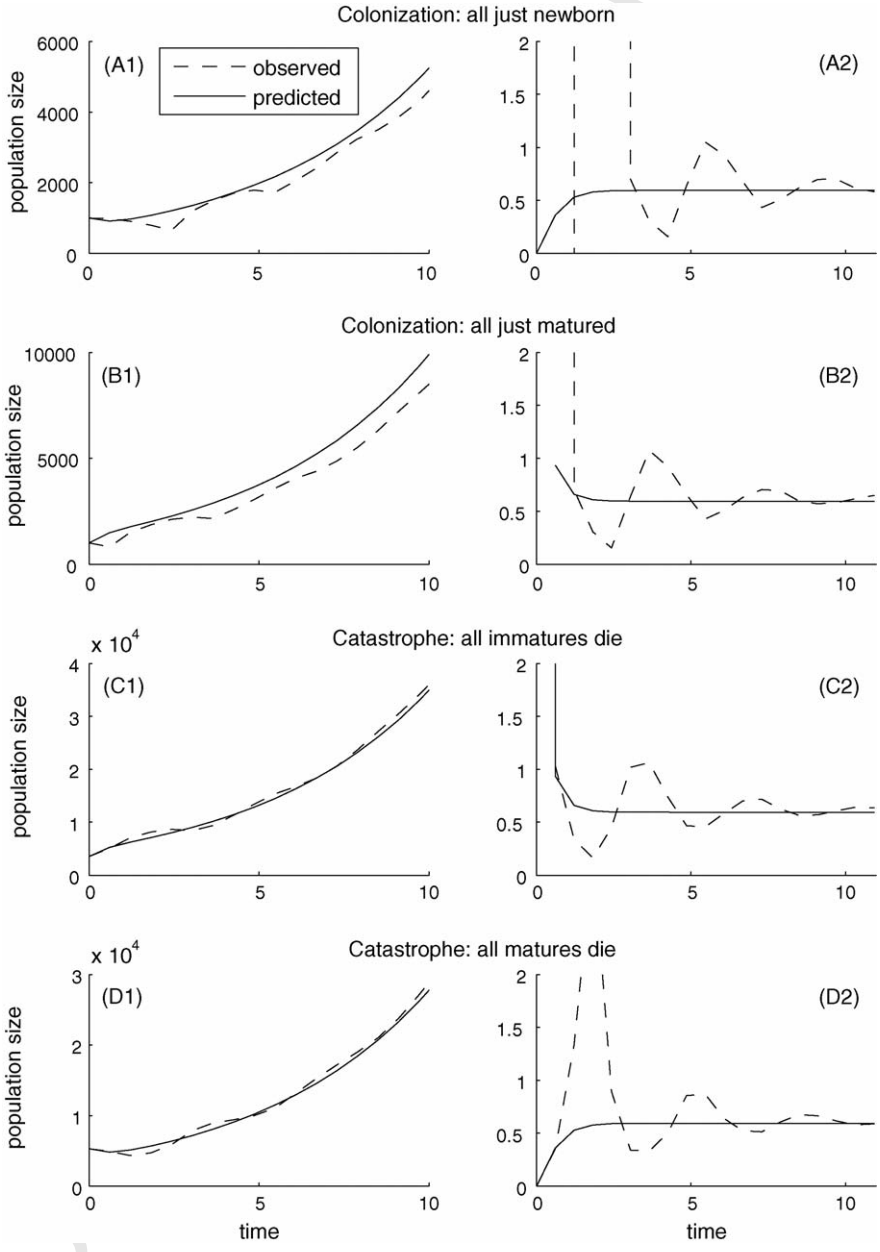

Fig. 11 – *Colonizations*. Plots: (A) initial population is comprised of newly born individuals. Population size (A1) and ratio of matures and immatures (A2) shown; (B) initial population is comprised of newly matured individuals. Population size (B1) and ratio of matures and immatures (B2) shown. *Catastrophes*. Plots: (C) all immatures die. Population size (C1) and ratio of matures and immatures (C2) shown; (D) all matures die. Population size (D1) and ratio of matures and immatures (D2) shown.

uals within a stage, i.e. individuals 'diffuse' throughout the stage. Therefore, the matrix model overestimates maturation following colonization by newborn individuals because a certain proportion of individuals in the matrix model matures at each projection interval, while in reality individuals must stay in the immature stage until age τ_p.

Both effects result in an overestimate of the number of newborns, and the matrix model predicts quicker-than-observed population recovery (Fig. 11). Adding more stages to the matrix model would help ameliorate both effects.

4. Discussion

The physiological responses of individuals to their environment determine their growth, survival and reproduction. In turn, these vital rates determine the dynamics of populations. In this paper, we have demonstrated how one can connect the physiological responses of individuals to population dynamics by constructing a matrix population model whose transition probabilities are determined by a DEB model. Although the analyses in this paper use a particular DEB model based on Kooijman's DEB theory, the developed framework (summarized in Appendix A) is general.

The construction process involved a number of approximations. To asses the impact of those approximations we compared the predictions of the matrix model to observations of an IBM whose individuals were governed by the DEB model. We found that, in general, predictions of the vital rates (fecundity, maturation probability, and survivorships) and of two asymptotic demographic statistics (population growth rate and stable stage distribution) closely matched the observations. Our approach tends to underestimate adult survivorship and overestimate fecundity. These mismatches are typically small, but are largest for rapidly declining populations. The mismatches can be attributed to two causes. First, it is difficult to estimate the vital rates from observations of the IBM when λ is small because the number of stage transitions observed before extinction is limited. Second, the pooling effect (discussed in Section 3) becomes more important when λ is small. This effect, present in other structured models (e.g. Nisbet et al., 1997), is caused by pooling the reproductive energy of organisms unable to reproduce individually into a common pool, which then provides enough energy to produce offspring.

In addition to comparisons of asymptotic statistics, we also compared transient population trajectories under a number of ecological scenarios. The match between the matrix-based predictions and the IBM-based observations were good when the initial age distribution within each stage was close to the stable distribution. However, when these distributions were not close, the matrix model poorly captured the transient dynamics, principally as a result of numerical diffusion (discussed in Section 3.3). The effects of numerical diffusion can typically be ameliorated by the inclusion of additional stages in the matrix model.

Many previous studies relate continuous-time physiological models to demographic models. For example, de Roos et al. (1992) connect size-dependent growth, mortality and reproduction, obtained from a physiological model, to demographic dynamics using escalator boxcar train technique (see also de Roos, 1988, 1997; de Roos et al., 1997). Ross et al. (1994) connect rudimentary zooplankton energy balance models to ecosystem dynamics using ordinary differential equations (see also Ross et al., 1993a,b), while Nisbet et al. (1997) use the same type of equations to represent biomass dynamics of a *Daphnia* population starting from partial differential equations for individual growth based on simple physiological considerations. Dougherty et al. (2002) link a physiological model of bacterial growth to population dynamics through ordinary differential equations representing sugar availability, acid concentrations and energy storage. McCauley et al. (1996) investigate dynamics of a stage-structured demographic model formulated using delay-differential equations starting from physiology of a herbivorous zooplankton (see also Gurney et al., 1983; Nisbet and Gurney, 1983; Nisbet et al., 1989). Kooi and Kooijman (1997) investigate differences between discrete and continuous approaches to reproduction by incorporating a DEB model into partial differential equations describing two physiological stages of their demographic model, and then using a finite difference scheme to project the population through time (see also Murphy, 1983; Metz and Diekmann, 1986; Kooijman et al., 1989). In addition to connecting a physiological model to the McKendrick–von Forester population conservation equation (Kot, 2001, pp. 391–400), Ault et al. (1999) add a spatial model to investigate population dynamics of sea trout and pink shrimp. These studies highlight the fact that there are demographic models other than matrix population models that we could have used.

Choices among these demographic models depend both on biological considerations – the life cycle of the organism, the form of the data, and the biological question at hand – and on the tastes of the scientist. Matrix models have several strengths. For many organisms, classification by stage is more useful than classification by age, and stage-classified models are particularly easy to develop in matrix form. In addition, matrix models are currently used in the theory of life history evolution more than other stage-structured models (Roff, 1992; Stearns, 1992), as an approximation to McKendrick–von Forester population equations (Kooi et al., 2001), as well as a way to incorporate toxic effects observed in individuals into demographic models (Lopes et al., 2005). We hope to use our modelling framework to address evolutionary questions at another time.

Our analyses in this paper is based on a specific κ-rule DEB model. The approach we use requires only the solutions of our individual model: size, energy committed to reproduction, energy needed to reproduce, and the risk of death as functions of age. The same approach can be used with any other κ-rule DEB model (Kooijman, 2000), as well as any other individual model that produces these outputs (e.g. von Bertalanffy, 1957; Kilgore and Armitage, 1978; Wunder, 1978; Paloheimo et al., 1982; Huntley et al., 1987 (review); Hallam et al., 1990; Markussen et al., 1990; Persson et al., 1998; Hickie et al., 2000).

The principal advantage of a κ-rule model is that it is a *supply-side model*, i.e. a model in which food availability determines the growth, survival and reproduction of individuals.[2]

[2] A *demand-side model*, in contrast, determines what the energy intake must have been to have produced a prescribed pattern of growth and reproduction.

As such, it enables us to analyze the interacting effects of physiology and environmental variability on population dynamics. We plan to investigate these interactions in the future.

Uncited references

Gurney et al. (1996), Gurney and Nisbet (1998), van Haren and Kooijman (1993)

Acknowledgments

We thank E. Montie for problems inspiring the project, and M. Hahn and S.A.L.M. Kooijman for insightful comments. The work of T. Klanjscek, H. Caswell and M. G. Neubert was supported by the David and Lucile Packard Foundation, the U.S. National Science Foundation (DEB-9973518, OCE-0083976), the U.S. Environmental Protection Agency (R-82908901) and the WHOI/MIT Joint Program in Biological Oceanography. R.M. Nisbet's work was supported by the STAR EaGLe program through the PEEIR Consortium (U.S. EPA R-882867601). WHOI contribution #.

Appendix A. Creating a matrix model based on a physiological model

1. Pick a projection interval α.
2. Obtain age-dependent size ($V(s)$), age-dependent commitment of reproductive energy ($\beta(s)$), and age-dependent probability of death conditioned on survival up to that age ($h(s)$) of an individual. For a DEB, use equations outlined in Table A.1.
3. Estimate energetic cost (C_N) of newborns.
4. Determine stages of the matrix model by dividing individuals into those younger than and older than the age at which individuals mature (τ_p).
5. Assume a growth rate λ_1, e.g.:

$$\lambda_1^{\text{assumed}} = 1. \tag{A.1}$$

6. Calculate the normalized stable age distribution using (15).
7. Calculate the transition probability (γ) using (19) or (18) in case of more than two stages.
8. Calculate survivorships (σ_i) for each stage using (21).
9. Calculate the average energy committed to reproduction per projection interval per mature individual from (22), the average number of newborns from (23), and the resulting fecundity (F) using (25).
10. Assemble the projection matrix using (10).
11. Calculate the maximum eigenvalue of the projection matrix, $\lambda_1^{\text{calculated}}$.
12. Repeat steps 6–12 with

$$\lambda_1^{\text{assumed}} = \lambda_1^{\text{calculated}}. \tag{A.2}$$

until satisfactory convergence of the growth rate is obtained. When $\lambda_1^{\text{calculated}}$ is very different from $\lambda_1^{\text{assumed}}$, the iterative process may be unstable because of possible overshoots that can lead to oscillations, rather than convergence. In such cases, in each iteration change $\lambda_1^{\text{assumed}}$ by only a fraction of the difference between $\lambda_1^{\text{assumed}}$ and $\lambda_1^{\text{calculated}}$ from the previous iteration.

Table A.1 – DEB model equations

Description	Equation no.
Rate of change of energy density	(1)
Rate of change of volume of the structure	(2)
Flux of energy committed to reproduction	(5)
Number of newborns in a breading season (for one female)	(26)
Rate of change of the hazard rate	(7)
Rate of accumulation of damage-inducing compounds	(8)

Appendix B. Calculating the stable age distribution

Let $N(s, t)$ be number of individuals of age s at time t. Then the total number of individuals at time t is

$$N_T(t) = \int_0^\infty N(s, t)\, ds, \tag{B.3}$$

and the age distribution:

$$\phi(s) = \frac{N(s, t)}{N_T(t)}. \tag{B.4}$$

From the definition of the hazard rate (6), we can calculate the probability that an individual survives to age s:

$$\phi_1(s) = \exp\left(-\int_0^s h(x)\, dx\right). \tag{B.5}$$

The number of individuals of age s at time t is, then, the number of individuals born at time $t - s$ that survived until the time t:

$$N(s, t) = N(0, t - s)\phi_1(s). \tag{B.6}$$

Furthermore, assuming the age distribution is constant and the intrinsic growth rate of the population r, the number of individuals of any age changes exponentially, so

$$N(s, t) = e^{-rs}N(s, t + s). \tag{B.7}$$

Inserting (B.6) and (B.7) into (B.4) gives:

$$\phi(s) = \frac{e^{-rs}N(0, t)\phi_1(s)}{N_T(t)}. \tag{B.8}$$

Since the age distribution is stable, the ratio of newborns to the total population is constant. Hence:

$$\phi(s) = Ke^{-rs}\phi_1(s). \tag{B.9}$$

Combining (B.5) and (14) with (B.9) and simplifying gives the stable age distribution (15).

REFERENCES

Ault, J.S., Luo, J., Smith, S.G., Serafy, J.E., Wang, D.J., Humston, R., Diaz, G.A., 1999. A spatial dynamic multistock production model. Can. J. Fish, Aquat. Sci. 56 (Suppl. 1), 4–25.

Caswell, H., 1989. Analysis of life table response experiments. 1. Decomposition of effects on population-growth rate. Ecol. Model. 46 (3/4), 221–237.

Caswell, H., 1996. Analysis of life table response experiments. 2. Alternative parameterizations for size- and stage-structured models. Ecol. Model. 88 (1–3), 73–82.

Caswell, H., 2001. Matrix population models: construction, analysis, and interpretation. Sinauer Associates, Sunderland, MA, USA. ISBN 0-87893-096-5.

de Roos, A.M., 1988. Numerical methods for structured population models: the escalator boxcar train. Numer. Methods Part. Diff. Eqs. 4, 173–195.

de Roos, A.M., Diekmann, O., Metz, J.A.J., 1992. Studying the dynamics of structured population models: a versatile technique and its application to Daphnia. Am. Nat. 139, 123–147.

de Roos, A.M., McCauley, E., Nisbet, R.M., Gurney, W.S.C., Murdoch, W.W., 1997. What individual life histories can (and cannot) tell about population dynamics. Aquat. Ecol. 31, 37–45.

de Roos, A.M., 1997. A gentle introduction to models of physiologically structured populations. In: Tuljapurkar, S., Caswell, H. (Eds.), Structured-population Models in Marine, Terrestrial, and Freshwater Systems. Chapman & Hall, New York, pp. 119–204.

Dougherty, D.P., Breidt Jr., F., McFeeters, R.F., Lubkin, S.R., 2002. Energy-based dynamic model for variable temperature batch fermentation by *Lactoccus lactis*. Appl. Environ. Microbiol. 2468–2478.

Fujiwara, M., Kendall, B.E., Nisbet, R.M., 2004. Growth autocorrelation and animal size variation. Ecol. Lett. 7, 106–113.

Gurney, W.S.C., Middleton, D.A.J., Nisbet, R.M., McCauley, E., Murdoch, W.W., de Roos, A.M., 1996. Individual energetics and the equilibrium demography of structured populations. Theor. Popul. Biol. 49, 344–368.

Gurney, W.S.C., Nisbet, R.M., Lawton, J.H., 1983. The systematic formulation of tractable single-species models incorporating age structure. J. Anim. Ecol. 52, 479–495.

Gurney, W.S.C., Nisbet, R.M., 1998. Ecological Dynamics. Oxford University Press, NY, USA.

Hallam, T.G., Lassiter, R.R., Li, J., Suarez, L.A., 1990. Modelling individuals employing an integrated energy response: application to Daphnia. Ecology 71 (3), 938–954.

Hickie, B.E., Kingsley, M.C.S., Hodson, P.V., Muir, C.G., Beland, P., Mackay, D., 2000. A modelling-based perspective on the past, present and future polychlorinated biphenyl contamination of the St. Lawrence beluga whale (*Delphinapterus leucas*) population. Can. J. Fish. Aquat. Sci. 57, 101–112.

Huntley, A.C., Costa, D.P., Worthy, G.A.J. & Castellini, M.A. (Eds.), 1987. Approaches to Marine Mammal Energetics. Society for Marine Mammalogy, Special Publication No. 1. Allen Press, USA.

Kilgore Jr., D.L., Armitage, K.B., 1978. Energetics of a yellow-bellied marmot population. Ecology 59, 78–88.

Kooi, B.W., Kooijman, S.A.L.M., 1997. Discrete event versus continuous approach to reproduction in structured population dynamics. Theor. Popul. Biol. 56, 91–105.

Kooi, B.W., Hallam, T.G., Kelpin, F.D.L., Krohn, C.M., Kooijman, S.A.L.M., 2001. Iteroparous reproduction strategies and population dynamics. Bull. Math. Biol. 63, 769–794.

Kooijman, S.A.L.M., 2000. Dynamic Energy and Mass Budgets in Biological Systems, 2nd ed. Cambridge University Press, Cambridge, UK. ISBN 0-521-78608-8.

Kooijman, S.A.L.M., Van Der Hoeven, N., Van Der Werf, D.C., 1989. Population consequences of a physiological model for individuals. Funct. Ecol. 3(3), 325–336.

Kot, M., 2001. Elements of Mathematical Ecology. Cambridge University Press, Cambridge, UK. ISBN 0-521-00150-1.

Lopes, C., Pery, A.R.R., Chaumot, A., Charles, S., 2005. Ecotoxicology and population dynamics: using DEBtox models in a Leslie modeling approach. Ecol. Model. 188 (1), 30–40.

Markussen, N.H., Ryg, M., Oritsland, N.A., 1990. Energy requirements for maintenance and growth of captive harbour seals, *Phoca Goenlandica*. Can. J. Zool. 68, 423–426.

McCauley, E., Roger, R.M., de Roos, A.M., Murdoch, W.W., Gurney, W.S.C., 1996. Structured population models of herbivorous zooplankton. Ecol. Monogr. 66 (4), 479–501.

Metz, J.A.J., Diekmann, O., 1986. The Dynamics of Physiologically Structured Populations. Lecture Notes in Biomathematics, vol. 68. Springer-Verlag, Berlin/NY.

Muller, E.B., Nisbet, R.M., 2000. Survival and production in variable resource environments. Bull. Math. Biol. 62, 1163–1189.

Murphy, L.F., 1983. A nonlinear growth mechanism in size structured population dynamics. J. Theor. Biol. 104, 493–506.

Nisbet, R.M., Gurney, W.S.C., 1983. The systematic formulation of population models for insects with dynamically varying instar duration. Theor. Popul. Biol. 23, 114–135.

Nisbet, R.M., Gurney, W.S.C., Murdoch, W.W., McCauley, E., 1989. Structured population models: a tool for linking effects at individual and population level. Biol. J. Linnean Soc. 37, 79–99.

Nisbet, R.M., McCauley, E., Gurney, W.S.C., Murdoch, W.W., de Roos, A.M., 1997. Simple representations of biomass dynamics in structured populations. In: Othmer, H.G., Adler, F.R., Lewis, M.A., Dallon, J.C. (Eds.), Case Studies in Mathematical Modeling—Ecology, Physiology, and Cell Biology. Prentice Hall, Upper Saddle River, NJ, pp. 61–79.

Nisbet, R.M., Muller, E.B., Lika, K., Kooijman, S.A.L.M., 2000. From molecules to ecosystems through dynamic energy budget models. J. Anim. Ecol. 69, 913–926.

Paloheimo, J.E., Crabtree, S.J., Taylor, W.D., 1982. Growth model of Daphnia. Can. J. Fish. Aquat. Sci. 39, 598–606.

Persson, L., Leonardsson, K., de Roos, A.M., Gyllenberg, M., Christensen, B., 1998. Ontogenetic scaling of foraging rates and the dynamics of a size-structured consumer-resource model. Theor. Popul. Biol. 54 (3), 270–293.

Ren, J.S., Ross, A.H., 2001. A dynamic energy budget model of the Pacific oyster *Crassostrea gigas*. Ecol. Model. 142 (1/2), 105–120.

Ripley, B.J., Caswell, H., in press. Recruitment variability and stochastic population growth of the soft-shell clam, *Mya arenaria*. Ecol. Model.

Ross, A.H., Gurney, W.S.C., Heath, M.R., 1993. Ecosystem models of Scottish sea lochs for assessing the impact of nutrient enrichment. ICES J. Mar. Sci. 50, 359–367.

Ross, A.H., Gurney, W.S.C., Heath, M.R., Hay, S.J., Henderson, E.W., 1993b. A strategic simulation model of a fjord ecosystem. Limnol. Oceanogr. 38, 128–153.

Ross, A.H., Gurney, W.S.C., Heath, M.R., 1994. A comparative study of the ecosystem dynamics of four fjords. Limnol. Oceanogr. 39, 318–343.

van Haren, R.J.F., Kooijman, S.A.L.M., 1993. Application of a dynamic energy budget model to *Mytilus edulis* (L.), Netherlands. J. Sea Res. 31 (2), 119–133.
von Bertalanffy, L., 1957. Quantitative laws in metabolism and growth. Q. Rev. Biol. 32 (3), 217–231.
Wunder, B.A., 1978. Implication of a conceptual model for the allocation of energy resources by small mammals. In: Snyder, O. (Ed.), Populations of Small Mammals under Natural Conditions. Pymatuning Laboratory of Ecology, University of Pittsburgh Special Publication Series 5, Pittsburgh, PA, p. 6875.